The Recombinant BCG Δ*ureC::hly* Vaccine Targets the AIM2 Inflammasome to Induce Autophagy and Inflammation

Hiroyuki Saiga,[1] Natalie Nieuwenhuizen,[1] Martin Gengenbacher,[1,a] Anne-Britta Koehler,[1] Stefanie Schuerer,[1] Pedro Moura-Alves,[1] Ina Wagner,[2] Hans-Joachim Mollenkopf,[2] Anca Dorhoi,[1] and Stefan H. E. Kaufmann[1]

[1]Department of Immunology and [2]Core Facility Microarray, Max Planck Institute for Infection Biology, Berlin, Germany

Background. The recombinant BCG Δ*ureC::hly* (rBCG) vaccine candidate induces improved protection against tuberculosis over parental BCG (pBCG) in preclinical studies and has successfully completed a phase 2a clinical trial. However, the mechanisms responsible for the superior vaccine efficacy of rBCG are still incompletely understood. Here, we investigated the underlying biological mechanisms elicited by the rBCG vaccine candidate relevant to its protective efficacy.

Methods. THP-1 macrophages were infected with pBCG or rBCG, and inflammasome activation and autophagy were evaluated. In addition, mice were vaccinated with pBCG or rBCG, and gene expression in the draining lymph nodes was analyzed by microarray at day 1 after vaccination.

Results. BCG-derived DNA was detected in the cytosol of rBCG-infected macrophages. rBCG infection was associated with enhanced absent in melanoma 2 (AIM2) inflammasome activation, increased activation of caspases and production of interleukin (IL)-1β and IL-18, as well as induction of AIM2-dependent and stimulator of interferon genes (STING)–dependent autophagy. Similarly, mice vaccinated with rBCG showed early increased expression of *Il-1β*, *Il-18*, and *Tmem173* (transmembrane protein 173; also known as STING).

Conclusions. rBCG stimulates AIM2 inflammasome activation and autophagy, suggesting that these cell-autonomous functions should be exploited for improved vaccine design.

Keywords. recombinant BCG Δ*ureC::hly*; macrophages; inflammasome; autophagy; innate immunity; vaccination; tuberculosis.

Tuberculosis, caused by the intracellular bacterium *Mycobacterium tuberculosis*, is a major infectious disease, causing 1.5 million deaths every year [1, 2]. BCG vaccine, created using *Mycobacterium bovis* bacille Calmette-Guérin (BCG), is the only licensed vaccine against tuberculosis. However, meta-analysis of published studies indicates that BCG only protects against severe forms of tuberculosis in infants and not against pulmonary tuberculosis in any age group [3, 4]. Therefore, novel vaccine candidates against tuberculosis are urgently needed.

In tuberculosis, macrophages serve as both habitat and first line of defense against *M. tuberculosis* [5]. Multiple pattern-recognition receptors sense mycobacterial molecular patterns at distinct subcellular sites of the macrophage. Toll-like receptors and C-type lectin receptors are sensors on the cell surface for extracellular mycobacterial components, while nucleotide-binding oligomerization domain-like receptors (NLRs) and aryl hydrocarbon receptor sense mycobacterial molecules in the host cytosol [6, 7]. Intracellular signaling cascades from these receptors induce production of proinflammatory cytokines, chemokines, and antimicrobial molecules and modulate cell death [8]. Importantly, macrophage-derived cytokines, such as tumor necrosis factor α (TNF-α), interleukin (IL)-12, and IL-1 family members, including IL-1β and IL-18, are critical for host defense against tuberculosis

Received 29 October 2014; accepted 1 December 2014; electronically published 11 December 2014.

[a]Present affiliation: Department of Microbiology, Yong Loo Lin School of Medicine, National University of Singapore.

Correspondence: Stefan H. E. Kaufmann, PhD, Max Planck Institute for Infection Biology, Department of Immunology, Charitéplatz 1, 10117 Berlin, Germany (kaufmann@mpiib-berlin.mpg.de).

The Journal of Infectious Diseases® 2015;211:1831–41

DOI: 10.1093/infdis/jiu675

[9]. Apoptosis of infected macrophages renders mycobacterial antigens accessible for processing and presentation, thereby contributing to stimulation of a protective T-cell response [10]. Activation of macrophages by these T cells controls the growth of *M. tuberculosis*. Thus, macrophages play a crucial role in protection against *M. tuberculosis* infection.

Inflammasomes, multiprotein platforms composed of intracellular sensors and caspase 1, are formed in the cytosol of innate immune cells such as macrophages and are primarily activated by pathogen-derived molecular patterns or host-derived danger molecules [11]. Inflammasome activation results in cleavage of the active form of caspase 1 and secretion of IL-1β and IL-18, whose proinflammatory activities direct host responses to infection [11]. Absent in melanoma 2 (AIM2) inflammasome senses cytosolic DNA [12, 13], and its activation plays a role in host defense against DNA viruses and intracellular bacteria such as listeriae and mycobacteria [14–16]. Moreover, the AIM2 inflammasome is involved in the induction of caspase 1–dependent cell death, termed "pyroptosis" [12], and recent studies suggest that AIM2 inflammasome induction in macrophages also triggers autophagy [17].

Autophagy is the major protein degradation process through which intracellular components, including cytosolic proteins and organelles, are disposed of during steady state [18]. Autophagy is induced by stress conditions such as starvation and bacterial infection [18] and has been demonstrated to contribute to innate immunity against mycobacteria [19–21]. Furthermore, autophagy leads to the delivery of antigens to major histocompatibility complex (MHC) molecules [22]. Thus, autophagy plays an important role in host defense both through enhanced antigen presentation to T cells and direct elimination of intracellular pathogens.

The recombinant vaccine candidate BCG Δ*ureC::hly* (rBCG) expresses the membrane-perforating listeriolysin O (Hly; encoded by the gene *hly*) of *Listeria monocytogenes* and is devoid of urease C, to prevent interference with phagosomal pH acidification [23]. It is the most advanced live vaccine candidate that has successfully passed 2a trial for safety in its target population, infants (clinical trials registration: NCT01479972) [24, 25]. In experimental mouse models, this rBCG vaccine induces superior protection against the laboratory strain *M. tuberculosis* H37Rv and the more virulent strain Beijing/W genotype family, when compared to parental BCG (pBCG) [23]. Furthermore, increased protection afforded by rBCG was shown to be associated with increased numbers of central memory T cells, increased T-helper type 17 (Th17) responses and earlier recruitment of antigen-specific T cells to the lungs [26, 27]. Superior rBCG-induced protection has been attributed to the translocation of vaccine antigens to the cytosol and to increased apoptosis of macrophages harboring rBCG [23, 25, 28, 29]. Nonetheless, additional biological processes likely contribute to the enhanced immunity induced by rBCG.

In this study, we analyzed early events in host cells after exposure to rBCG. rBCG, but not pBCG, induced AIM2 inflammasome activation and autophagy. Consequently, activation of caspases and production of IL-1β and IL-18 were elevated in human macrophages harboring rBCG. Similarly, *Il-1β* and *Il-18* transcripts were significantly increased in mice vaccinated with rBCG, compared with unvaccinated mice, but levels in pBCG recipients did not differ from those in unvaccinated mice. These findings elucidate mechanisms underlying enhanced innate immune responses to rBCG. It is tempting to speculate that this could provide a possible mechanistic explanation for improved protective immunity induced by rBCG, compared with immunity induced by pBCG. These mechanisms could also be exploited for the design of other vaccine candidates against tuberculosis or other infectious diseases.

MATERIALS AND METHODS

Cells and Bacteria

Human monocytic cell line THP-1 cells were cultured in Roswell Park Memorial Institute (RPMI) 1640 medium (Gibco) containing 10% heat-inactivated fetal bovine serum, 10 mM HEPES buffer solution, 1 mM sodium pyruvate, and 2 mM L-glutamine. THP-1 monocytic cells were differentiated into macrophages in RPMI 1640 medium containing 5 ng/mL PMA (Sigma) for 48 hours. pBCG/rBCG (BCG Prague background [25]) and Ds-Red pBCG/rBCG were cultured in Middlebrook 7H9-ADC medium. Fluorescent protein-expressing strains were generated using the integrative vector pMV306 [30]. The Ds-Red gene under control of the constitutive BCG *hsp60* promoter was inserted into the *Xba*I/*Hind*III sites of pMV306 and subsequently introduced into pBCG and rBCG by electroporation. Transformants were selected on Middlebrook 7H11-OADC agar/50 μg/mL kanamycin.

Caspase Activity

THP-1 macrophages were infected with Ds-Red pBCG/rBCG (multiplicity of infection [MOI], 5) for 3 hours, and then vigorously washed with phosphate-buffered saline (PBS) to eliminate extracellular BCG. After 48 hours, activated caspase was labeled by the FAM-FLICA in vitro caspase detection kit according to the manufacturer's instructions (Immuno Chemistry). Stained cells were mounted with ProLong Gold antifade reagent (Life Technologies) on glass slides and analyzed using a fluorescence microscope (Leica TCS SP8).

Isolation of Bacterial DNA From Cytosolic Fraction and Polymerase Chain Reaction (PCR) Amplification

THP-1 macrophages were infected with pBCG/rBCG at MOIs of 10 and 30. After 3 hours, cells were vigorously washed with PBS, and the cytosolic fraction was then isolated by the Qproteome Cell Compartment Kit, following the manufacturer's

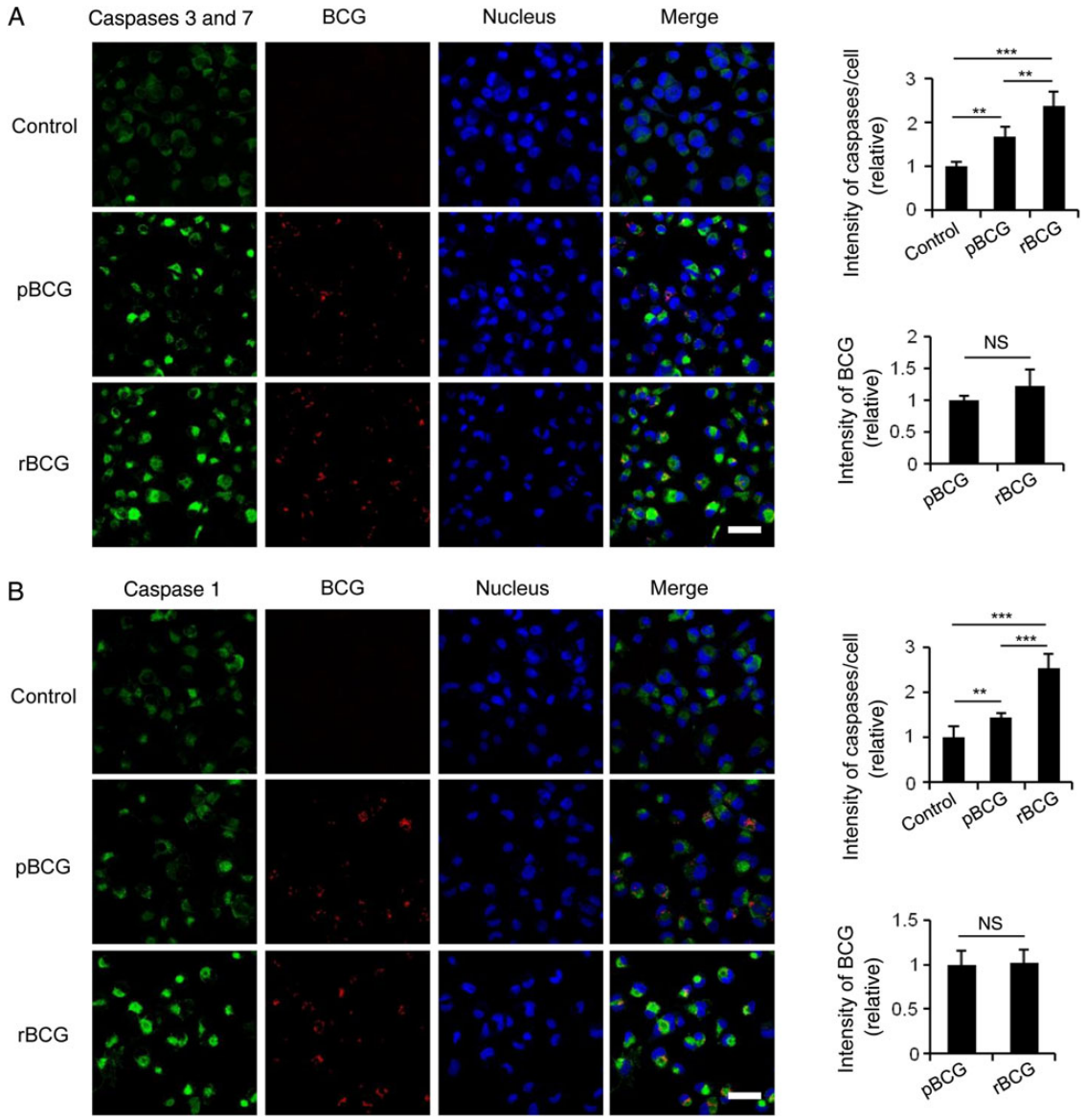

Figure 1. Activation of caspases 3 and 7 (*A*) and caspase 1 (*B*) by recombinant bacille Calmette-Guérin Δ*ureC::hly* (rBCG). THP-1 macrophages were infected with Ds-Red parental BCG (pBCG) or Ds-Red rBCG (multiplicity of infection, 5; red) for 48 hours, and activated caspases (green) and nucleus (blue) were monitored by immunofluorescence. Scale bar represents 50 μm. Fluorescence intensities of caspases and BCG were determined in an average of 9 random fields, using ImageJ software. Data are representative of 3 independent experiments. $^{**}P < .01$ and $^{***}P < .005$. Abbreviation: NS, not significant.

instructions (Qiagen). To extract bacterial DNA, BCG (1×10^7 colony-forming units [CFU]) was boiled for 10 minutes, and supernatants were collected by centrifugation. PCR amplification was performed with GoTaq DNA Polymerase (Promega) and 20 ng of each DNA as template.

Immunoprecipitation and Immunoblot Analysis

THP-1 macrophages were stimulated with 500 ng/mL lipopolysaccharide (LPS) for 3 hours and then transfected with poly(dA:dT) (Sigma) using Lipofectamine 2000 (Life Technologies). Cells were infected with pBCG/rBCG (MOI, 10) for 3 hours and washed with PBS. After 24 hours, supernatants were precleared with protein G Sepharose (GE Healthcare) and then incubated with anti-caspase 1 p20 rabbit antibody (Cell Signaling Technology). Cell pellets were lysed in radioimmunoprecipitation assay buffer (Millipore). Samples were separated by sodium dodecyl sulfate polyacrylamide gel electrophoresis (SDS-PAGE) and transferred to polyvinylidene difluoride (PVDF) membranes. Membranes were incubated with anti-caspase 1 p20 antibody and anti–β-actin antibody (Sigma).

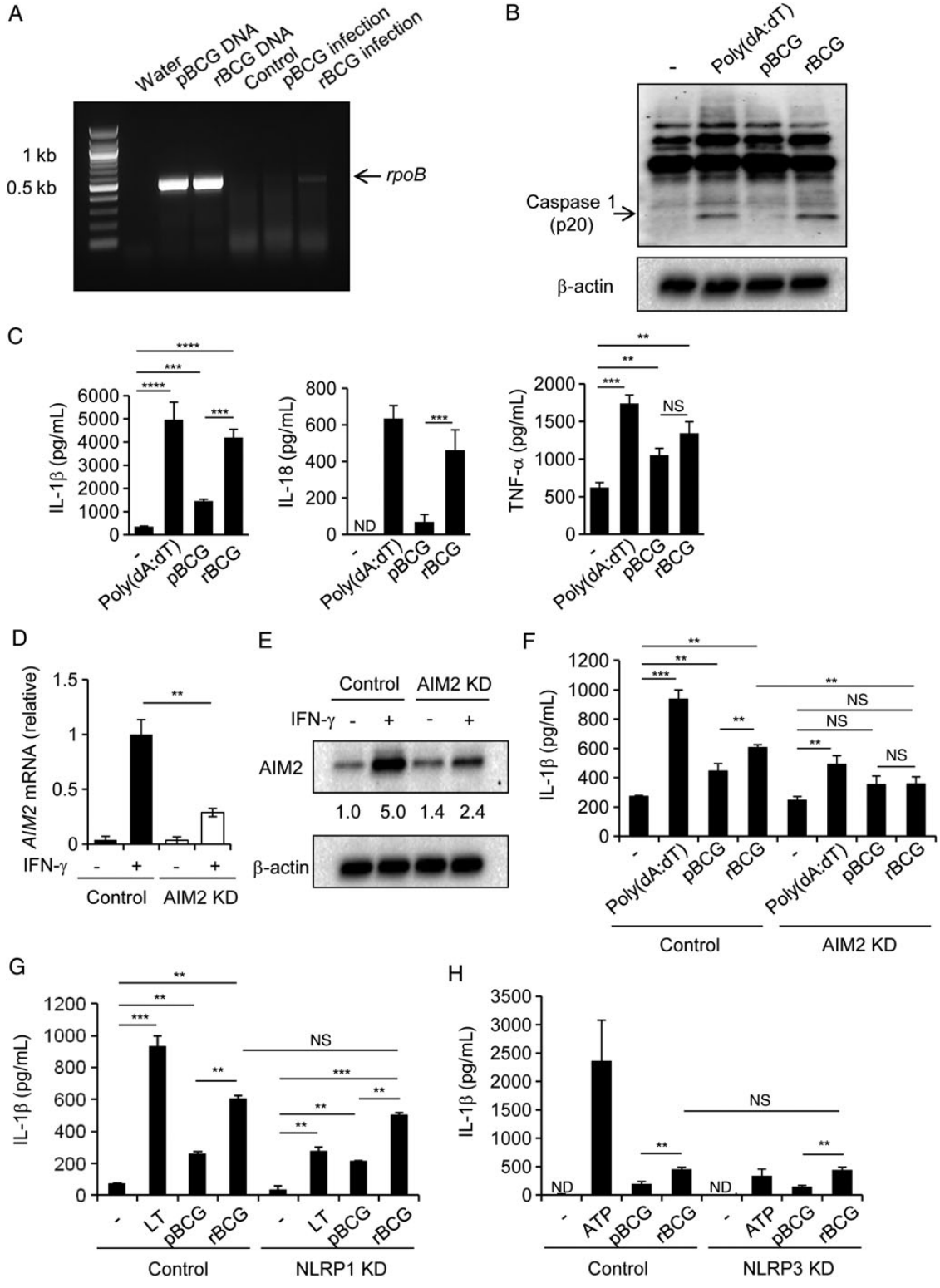

Figure 2. Absent in melanoma 2 (AIM2)–dependent inflammasome activation by recombinant bacille Calmette-Guérin Δ*ureC::hly* (rBCG). *A*, THP-1 macrophages were infected with parental BCG (pBCG) or rBCG (multiplicity of infection [MOI], 10) for 3 hours, and bacterial DNA was isolated from purified cytosolic fraction. The target gene *rpoB* was detected by polymerase chain reaction (PCR) analysis. Data are representative of 3 independent experiments. *B*, THP-1 macrophages were primed with 500 ng/mL lipopolysaccharide (LPS) for 3 hours and then transfected with poly(dA:dT) for 12 hours or infected with pBCG or rBCG (MOI, 10) for 24 hours. Supernatants were immunoprecipitated, and caspase 1–specific bands were detected by Western blot. β-actin was used as control for cell lysates. Data are representative of 3 independent experiments. *C*, THP-1 macrophages were primed with 500 ng/mL LPS for 3 hours and then transfected with poly(dA:dT) for 24 hours or infected with pBCG or rBCG (MOI, 20) for 24 hours. Levels of the indicated cytokines in the culture supernatants were measured by enzyme-linked immunosorbent assay (ELISA). Data are representative of 3 independent experiments. *D*, AIM2 knockdown

Enzyme-Linked Immunosorbent Assay (ELISA)

Levels of IL-1β and TNF-α in culture supernatants were measured by ELISA, following manufacturer's instructions (R&D Systems). The ELISA kit for IL-18 was purchased from Medical & Biological Laboratories.

Production of Knockdown Cells

Lentiviruses were produced according to TRC lentiviral proceedings (https://www.broadinstitute.org/genome_ bio/trc/publicProtocols.html). Briefly, HEK 293T cells were transfected with lentiviral packaging mix (Sigma) and 100 ng of the short hairpin RNA (shRNA) containing pLKO.1-puro vector (Sigma), using Fugene 6 (Roche). Lentiviral infection was performed according to protocols available at the RNAi Consortium website (https://www.broadinstitute.org/genome_bio/trc/publicProtocols.html). Briefly, THP-1 cells were resuspended in medium containing 8 μg/mL of polybrene (Sigma), and 10 μL of lentivirus was added to the cells. Transduced cells were further selected using 5 μg/mL puromycin (Calbiochem). Total RNA was isolated with Trizol reagent (Invitrogen) and then reverse transcribed using the iScript cDNA Synthesis Kit (Bio Rad). Quantitative real-time PCR was performed using SYBR Green sequence primers. Data are shown as relative messenger RNA levels normalized by corresponding GAPDH level. Immunoblot analysis was performed using anti-AIM2 antibody (Cell Signaling Technology).

Analysis of Endogenous LC3

THP-1 macrophages were cultured in RPMI 1640 medium containing 10 μg/mL E64d and 10 μg/mL pepstatin A (Sigma) [31]. Cells were stimulated with 25 μg/mL rapamycin (Sigma) or infected with pBCG/rBCG (MOI, 10). After 3 hours, cells were washed with PBS and then lysed in cell lysis solution (2% Triton X-100 and Complete Protease Inhibitor Cocktail, Roche) at 4°C for 30 minutes for immunoblot analysis. Supernatants of centrifuged lysates were separated by SDS-PAGE and transferred to PVDF membranes. Membranes were incubated with anti–LC3-II antibody (Medical & Biological Laboratories) and anti–β-actin antibody. For immunofluorescence analysis, treated cells were fixed with 4% paraformaldehyde and permeabilized with 0.3% Triton X-100, and blocking was performed with 1% bovine serum albumin. Cells were incubated with anti–LC3-II antibody at room temperature for 1 hour and then incubated with Alexa 488 anti–rabbit IgG antibody (Life Technologies) for 30 minutes.

Mouse Experiments

All mouse experiments were approved by and conducted in accordance with guidelines of the State Office for Health and Social Services (Landesamt für Gesundheit und Soziales), Berlin, Germany. Female C57BL/6 mice (8–10 weeks old) were purchased from Charles River Laboratories (Germany). Mice were kept under specific pathogen-free conditions. Vaccines (1×10^6 CFU BCG or rBCG in 100 μL PBS) were delivered subcutaneously at the tail base (n = 5 mice per group). At 24 hours after vaccination, mice were killed, and draining lymph nodes were collected in the RNA-stabilization reagent RNAlater (Qiagen) and frozen. Preserved lymph nodes were added to Trizol reagent, and phenol chloroform extraction was performed. RNA quality was ensured using the Bioanalyzer instrument. Agilent whole mouse genome microarrays were performed using the RNA samples.

Statistical Analysis

The statistical significance of in vitro data was evaluated using either the Student *t* test or 1-way analysis of variance (ANOVA) and the Bonferroni posttest for multiple measurements. In vivo data were analyzed using Genespring 12.6 GX (Agilent Technologies), with quality control filters, normalization, and 1-way ANOVA. *P* values of $< .05$ were considered statistically significant.

RESULTS

rBCG Is a Potent Activator of Caspase 3, Caspase 7, and Caspase 1

Previous studies analyzed mechanisms underlying improved $CD4^+$ and $CD8^+$ T-cell responses induced by rBCG [23, 25, 28, 29]. Since various processes involved in cell death, including apoptosis, are controlled by caspases [32], we investigated

Figure 2 continued. (KD) THP-1 cells were generated using lentiviruses encoding short hairpin RNAs (shRNAs). To determine KD efficiency, scramble control and AIM2 KD cells were stimulated with 60 ng/mL interferon γ (IFN-γ) for 24 hours, and then quantitative real-time PCR was performed. Data are representative of 2 independent experiments. *E*, IFN-γ–treated cell pellets were lysed, and protein expression was detected by Western blot. The quantification of band intensity was performed using ImageJ software. Data are representative of 2 independent experiments. *F*, Scramble control and AIM2 KD THP-1 macrophages were primed with 500 ng/mL LPS for 3 hours and then transfected with poly(dA:dT) for 24 hours or infected with pBCG or rBCG (MOI, 20) for 24 hours. Abundances of interleukin 1β (IL-1β) in culture supernatants were measured by ELISA. Data are representative of 3 independent experiments. *G*, nucleotide-binding oligomerization domain like receptor pyrin domain-containing 1 (NLRP1) KD THP-1 cells were generated using lentiviruses encoding shRNAs. Scramble control and NLRP1 KD THP-1 macrophages were primed with 500 ng/mL LPS for 3 hours and then stimulated with 1 μg/mL lethal toxin (LT) for 6 hours or infected with pBCG or rBCG (MOI, 20) for 24 hours. Abundances of IL-1β in culture supernatants were measured by ELISA. Data are representative of 2 independent experiments. *H*, NLRP3 KD THP-1 cells were generated using lentiviruses encoding shRNAs. Scramble control and NLRP3 KD THP-1 macrophages were primed with 500 ng/mL LPS for 3 hours and then stimulated with 5 mM ATP for 20 minutes or infected with pBCG or rBCG (MOI, 20) for 24 hours. Abundances of IL-1β in culture supernatants were measured by ELISA. Data are representative of 2 independent experiments. $^{**}P < .01$, $^{***}P < .005$, and $^{****}P < .001$. Abbreviations: IL, interleukin; ND, not detected; NS, not significant; TNF-α, tumor necrosis factor α.

whether rBCG induced their activation. Differentiated THP-1 cells were infected with Ds-Red fluorescently labeled bacteria, either pBCG or rBCG, and subsequently caspase activity was measured (Supplementary Figure 1*A*). Polycaspase activity was significantly increased in cells harboring rBCG cells, compared with pBCG samples, while naive macrophages exhibited scant staining. Thus, rBCG showed superior broad caspase activation over pBCG.

Next, we determined which caspases were activated by rBCG. Caspase 3 and 7, also known as apoptotic effector caspases [32], were highly activated by rBCG (Figure 1*A*). In contrast, the apoptotic initiator caspase 8 [32] was not activated after infection with either BCG strain (Supplementary Figure 1*B*). Finally, we monitored the activation of caspase 1, which is an important regulator of the inflammatory response [33]. Caspase 1 activity was markedly increased in macrophages harboring rBCG (Figure 1*B*). Overall, rBCG induced heightened activation of distinct caspases, compared with pBCG. Of note is the increased caspase 1 activity, suggesting a propensity for rBCG to initiate more-potent inflammation.

rBCG DNA Is Released Into the Host Cytosol

Initial investigations on the modus operandi of rBCG unveiled increased presence of antigens in the cytosol of macrophages harboring this vaccine strain, compared with those harboring pBCG [23, 29]. While neither pBCG nor rBCG was found to egress into the cytosol, other intracellular bacteria, such as *M. tuberculosis* and *L. monocytogenes*, have been shown to escape from the phagosome into the cytosol [29, 34–36], promoting the presence of cytosolic bacterial DNA [15, 37]. We determined whether DNA from rBCG or pBCG was released into the cytosol despite the bacteria remaining in the phagosome. The presence of BCG-derived DNA in the cytosolic fraction was determined by PCR, using primers specific for the mycobacterial gene encoding the β subunit of RNA polymerase (*rpoB*) gene, which is conserved in all mycobacteria [38] (Figure 2*A* and Table 1). *rpoB* transcripts were demonstrable in the cytosolic fraction of rBCG-infected macrophages, but not in pBCG-infected or uninfected macrophages, at a MOI of 10 (Figure 2*A*) and a MOI of 30 (data not shown). Hence, rBCG promoted mycobacterial DNA release into the cytosol, whereas pBCG failed to do so at detectable levels.

rBCG Activates the AIM2 Inflammasome

In view of the remarkable activation of caspase 1 and the presence of mycobacterial DNA within the cytosol of rBCG-infected macrophages, we hypothesized that rBCG may activate the inflammasome via the cytosolic DNA sensor AIM2. Inflammasome activation was first analyzed by Western blot of caspase 1 (Figure 2*B*). The active caspase 1 (p20) was not detected in uninfected and pBCG-infected macrophages. In contrast, rBCG or stimulation with synthetic B-form double-stranded DNA (poly[dA:dT]) resulted in cleavage of the p20 form of caspase 1. Since the active form of caspase 1 has been shown to mediate the secretion of the cytokines IL-1β and IL-18 [11], we next analyzed the secretion of IL-1β and IL-18 after BCG infection (Figure 2*C*). Production of IL-1β and IL-18 was markedly increased after rBCG infection, compared with pBCG infection. In contrast, both pBCG and rBCG induced TNF-α secretion at comparable abundance.

Table 1. Polymerase Chain Reaction (PCR) Primer Sequences and Quantitative Real-time PCR Primer Sequences

PCR primer sequences
rpoB forward, 5′ -GCTGGACATCTACCGCAAGCTGC- 3′
rpoB reverse, 5′ -CAGCGGGTTCTGGTCCATG- 3′
Quantitative real-time PCR primer sequences
GAPDH forward, 5′-CATGAGAAGTATGACAACAGCCT-3′
GAPDH reverse, 5′-AGTCCTTCCACGATACCAAAGT-3′
AIM2 forward, 5′-CATCTGCAGCCATCAGAAAT-3′
AIM2 reverse, 5′-CGCTTCTGAAACCCTTCTCT-3′
GBP2 forward, 5′-TTGACAGAGCCTGGACGTTGG-3′
GBP2 reverse, 5′-AGGGTGTTGTTCCCCAGGTCAGA-3′
GBP5 forward, 5′-GGCCTCCGCTGCATACAAATCA-3′
GBP5 reverse, 5′-AACAGAGAAGCCCTTGTTCTTCCCA-3′

Next, we assessed the involvement of AIM2 in rBCG-induced inflammasome activation. AIM2 knockdown THP-1 cells were generated (Table 2), and knockdown efficiency was evaluated by quantitative real-time PCR and Western blot (Figure 2*D* and 2*E*; Table 1). Control and AIM2 knockdown macrophages were infected with pBCG or rBCG, and secretion of IL-1β was determined by ELISA (Figure 2*F*). As previously observed, rBCG induced higher IL-1β secretion as compared to pBCG. In contrast, levels of secreted IL-1β were lower in rBCG-infected AIM2 knockdown cells, compared with control cells, and were similar to those observed in pBCG-infected cells. Knockdown of other members of the inflammasome family, NLR pyrin domain–containing 1 (NLRP1) and NLRP3, did not influence IL-1β production by rBCG macrophages (Figure 2*G* and 2*H*). We conclude that rBCG activated the inflammasome in an AIM2-dependent manner, resulting in higher IL-1β secretion.

rBCG Induces Autophagy in Macrophages

Based on previous findings showing that activation of the AIM2 inflammasome stimulates autophagy [17], we investigated whether rBCG induced autophagy through this pathway. First, THP-1 macrophages were transfected with poly(dA:dT), and protein levels of the autophagy marker LC3-II were analyzed (Supplementary Figure 2). As expected, LC3-II levels were strongly increased in poly(dA:dT)-transfected control macrophages, but not AIM2 knockdown macrophages. Next, differentiated THP-1 cells were infected with pBCG or rBCG, and LC3-II levels were detected by Western blot (Figure 3*A*).

Table 2. Short Hairpin RNA Sequences

Sequence
AIM2
1. CCGGCCAACTGGTCTAAGCAGCATTCTCGAGAATGCTGCTTAGACCAGTTGGTTTTTG
2. CCGGCCCGCTGAACATTATCAGAAACTCGAGTTTCTGATAATGTTCAGCGGGTTTTTG
3. CCGGGCCACTAAGTCAAGCTGAAATCTCGAGATTTCAGCTTGACTTAGTGGCTTTTTG
4. CCGGAGCCACTAAGTCAAGCTGAAACTCGAGTTTCAGCTTGACTTAGTGGCTTTTTTG
5. CCGGCTGGAGTTCATAGCACCATAACTCGAGTTATGGTGCTATGAACTCCAGTTTTTG
NLRP1
1. CCGGCGTTTCCTATTGGGCCTGTTACTCGAGTAACAGGCCCAATAGGAAACGTTTTTTG
2. CCGGCCCTTCTTTGGGTCTCAGTTTCTCGAGAAACTGAGACCCAAAGAAGGGTTTTTTG
3. CCGGCTCATCTTCAGCAGACGGAAACTCGAGTTTCCGTCTGCTGAAGATGAGTTTTTTG
4. CCGGCGGTGACCGTTGAGATTGAATCTCGAGATTCAATCTCAACGGTCACCGTTTTTTG
NLRP3
1. CCGGCCGTAAGAAGTACAGAAAGTACTCGAGTACTTTCTGTACTTCTTACGGTTTTTG
2. CCGGCCAGCCAGAGTCTAACTGAATCTCGAGATTCAGTTAGACTCTGGCTGGTTTTTG
3. CCGGCCACAGTGTAACCTGCAGAAACTCGAGTTTCTGCAGGTTACACTGTGGTTTTTG
4. CCGGGCGTTAGAAACACTTCAAGAACTCGAGTTCTTGAAGTGTTTCTAACGCTTTTTG
5. CCGGGCTGGAATTGTTCTACTGTTTCTCGAGAAACAGTAGAACAATTCCAGCTTTTTG
STING
1. CCGGCATGGTCATATTACATCGGATCTCGAGATCCGATGTAATATGACCATGTTTTTTG
2. CCGGGCATGGTCATATTACATCGGACTCGAGTCCGATGTAATATGACCATGCTTTTTTG
3. CCGGGCTGGCATGGTCATATTACATCTCGAGATGTAATATGACCATGCCAGCTTTTTTG
4. CCGGGTCCAGGACTTGACATCTTAACTCGAGTTAAGATGTCAAGTCCTGGACTTTTTTG
5. CCGGGCCCGGATTCGAACTTACAATCTCGAGATTGTAAGTTCGAATCCGGGCTTTTTTG
Scramble
CAACAAGATGAAGAGCACCAA

While pBCG increased the abundance of LC3-II over controls only marginally, rBCG induced profound levels of LC3-II. Consistent with this finding, ratios of LC3-II puncta-positive cells and the intensity of the LC3-II signal, analyzed by immunofluorescence, were significantly higher after rBCG infection than after pBCG infection (Figure 3*B*). In contrast, there was no significant difference in LC3-II levels and ratios of LC3-II puncta-positive cells between pBCG-infected and rBCG-infected AIM2 knockdown macrophages (Figure 3*C* and 3*D*), while rapamycin-induced LC3-II levels were AIM2 independent. Recent studies suggest that stimulator of IFN genes (STING; also known as transmembrane protein 173) is an essential adaptor protein in the induction of autophagy by cytosolic DNA [37, 39]. Consistent with this notion, in STING knockdown macrophages, the heightened LC3-II signal in response to rBCG was no longer observed (Figure 3*E* and 3*F*). Therefore, rBCG likely triggered autophagy through both AIM2 and STING pathways.

Increased Expression of *Il-1β* and *Il-18* in rBCG-Vaccinated Mice

We investigated whether rBCG induced similar genes in vivo to those triggered in infected THP-1 macrophages. To this end, we analyzed gene expression in the draining lymph nodes of mice vaccinated with pBCG and rBCG at 24 hours after vaccination. After vaccination with rBCG, 96 hits (including genes, hypothetical genes, and long noncoding RNAs) were upregulated (defined as ≥2-fold differential expression; $P < .05$), compared with unvaccinated mice (Figure 4*A*). In contrast, only 38 hits were significantly upregulated after pBCG vaccination. Pathway analysis of genes upregulated exclusively after rBCG vaccination revealed enrichment of genes associated with innate immunity, including the IL-1 signaling pathway (Table 3). In rBCG-vaccinated mice, expression of *Il-18*, *Il-1β*, and *Myd88* (the gene encoding myeloid differentiation primary response 88), which was previously shown to be involved in IL-1 and IL-18 pathways [40], were significantly upregulated over expression in unvaccinated mice or mice vaccinated with pBCG (Figure 4*B*). These results suggest that both cytokines were critical immune regulators specifically induced by rBCG vaccination, as well as by in vitro challenge. Although we found no significant difference in expression of *Aim2* in mice vaccinated with rBCG, compared with unvaccinated controls (data not shown), genes encoding AIM2-related proteins, such as IFN-inducible 204 (*Ifi204*) and pyrin domain containing 4 (*Pydc4*) [41], and the gene encoding STING (*Tmem173*) were significantly upregulated. Thus, in vivo gene expression profiles after vaccination of mice supported our in vitro data with macrophages.

DISCUSSION

The recombinant BCG vaccine candidate, which expresses *hly* and is devoid of functional urease C (rBCG Δ*ureC::hly*), has been shown to induce improved protection over pBCG [23], but the underlying mechanisms are still incompletely understood. In the present study, we demonstrate that elevated levels of caspases 3 and 7, but not caspase 8, were induced by rBCG. This finding suggests that caspases 3 and 7 were induced in a process independent from initiator caspases. Caspases 3 and 7 can be directly processed by caspase 1 in vitro [42], and inflammasome-dependent caspase 1 activation induced by microbial stimuli and bacterial infection is essential for caspase 7 processing in macrophages [43]. Since our data reveal that rBCG activated the AIM2 inflammasome and, therefore, caspase 1, we

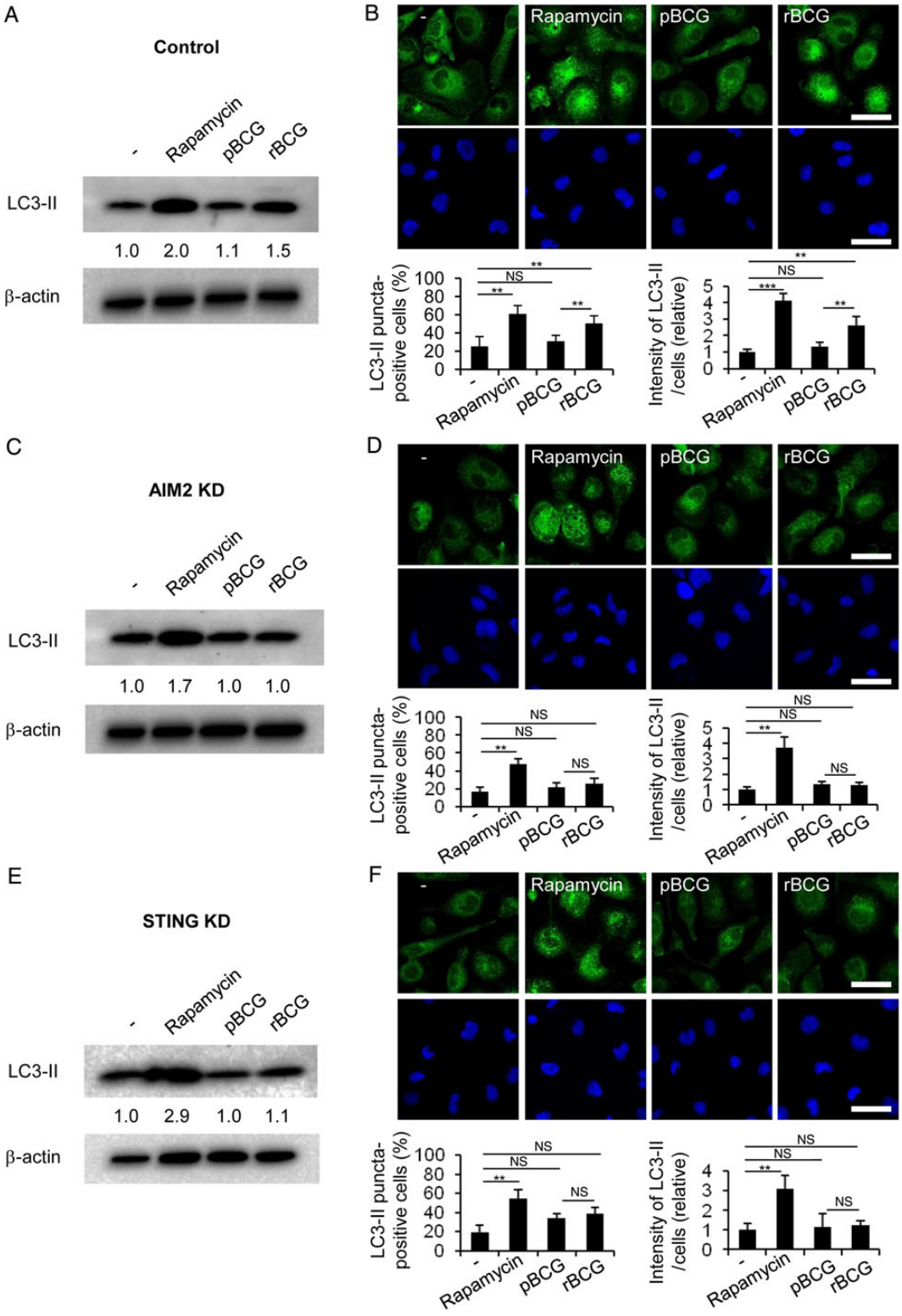

Figure 3. Induction of autophagy by recombinant bacille Calmette-Guérin Δ*ureC::hly* (rBCG). *A*, *C*, *E*, Scramble control (*A*), absent in melanoma 2 (AIM2) knockdown (KD; *C*), or stimulator of IFN genes (STING) KD (*E*) THP-1 macrophages were stimulated with rapamycin or infected with parental BCG (pBCG) or rBCG (multiplicity of infection [MOI], 10) for 3 hours. Cell pellets were lysed, and LC3-II–specific bands were detected by Western blot. β-actin was used as a control for cell lysates. The quantification of band intensity was performed using ImageJ software. Data are representative of 3 independent experiments. *B*, *D*, *F*, Scramble control (*B*), AIM2 KD (*D*), or STING KD (*F*) THP-1 macrophages were stimulated with rapamycin or infected with pBCG or rBCG (MOI, 10) for 3 hours. Cells were stained with antibody to LC3-II (green) and nucleus (blue). Scale bar represents 20 μm. Ratios of LC3-II puncta-positive cells and intensity of LC3-II signal were determined in an average of 9 random fields, using ImageJ software. Data are representative of 3 independent experiments. $^{**}P < .01$ and $^{***}P < .005$. Abbreviation: NS, not significant.

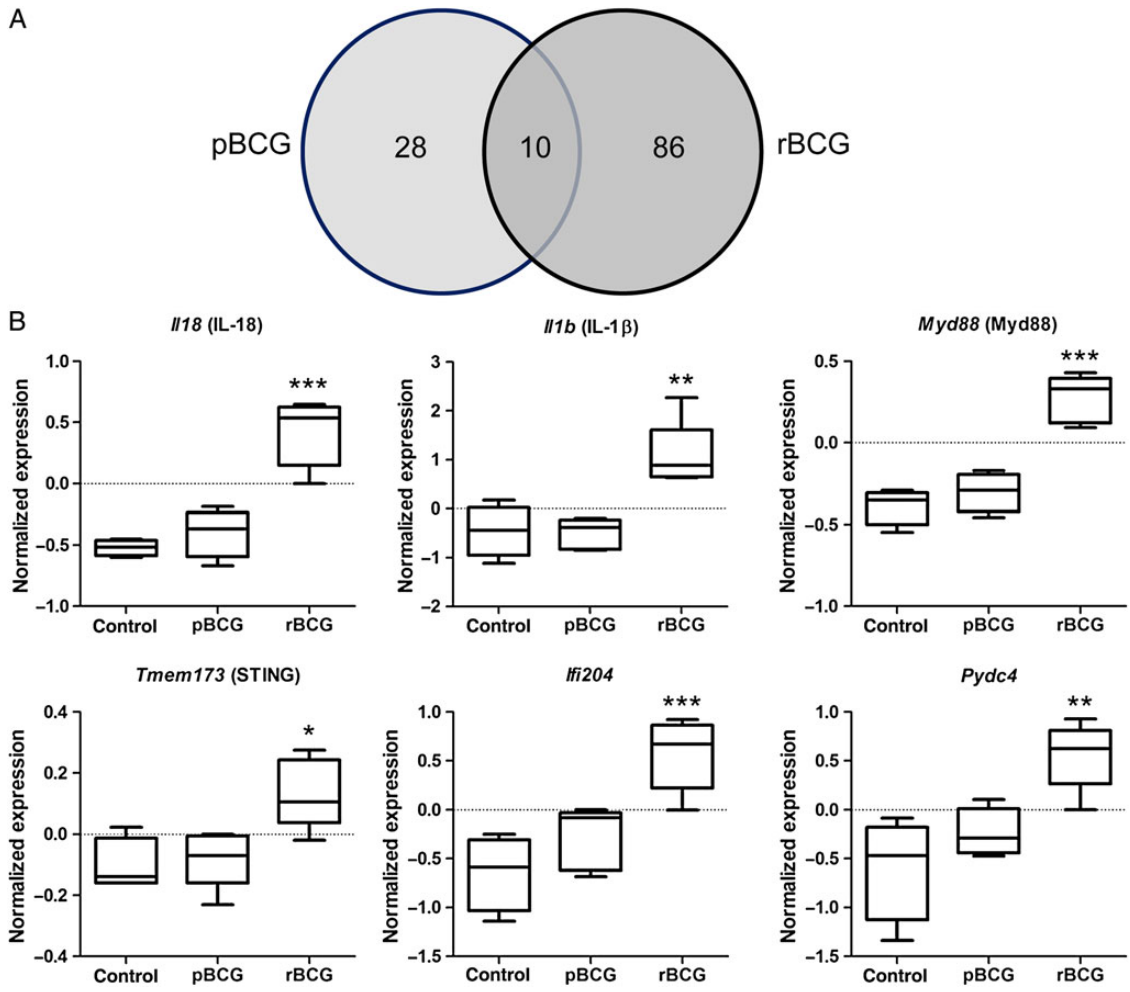

Figure 4. Upregulation of *Il-1β* and *Il-18* expression in draining lymph nodes of mice after vaccination with recombinant bacille Calmette-Guérin Δ*ureC::hly* (rBCG). *A*, Venn diagram of differentially upregulated genes 24 hours after vaccination, compared with unvaccinated mice. *B*, Normalized expression of the genes *Il-18* (gene encoding interleukin 18), *Il-1β* (gene encoding interleukin 1β), *Myd88* (gene encoding myeloid differentiation primary response), *Tmem173* (gene encoding transmembrane protein 173 [also known as stimulator of IFN gene {STING}]), *Ifi204* (gene encoding interferon-inducible 204), and *Pydc4* (gene encoding pyrin domain-containing 4) 24 hours after vaccination. **P* < .05, ***P* < .01, and ****P* < .005. Abbreviation: pBCG, parental BCG.

speculate that increased activation of effector caspases, caspases 3 and 7, in response to rBCG was mediated via caspase 1, as previously reported [43].

In support of the critical role of the AIM2 inflammasome for the superior caspase 1 activation and subsequent IL-1β release by macrophages harboring rBCG, we identified mycobacterial DNA as its potential ligand in the cytosol. Previous studies have revealed that *M. tuberculosis* is capable of egressing from the phagosome into the cytosol, whereas BCG remains in the phagosome, and that this mechanism has been considered the basis for $CD8^+$ T-cell stimulation by *M. tuberculosis* [35, 44, 45]. *Mycobacterium marinum* has also been shown to egress from the phagosome into the cytosol in a region of difference 1 (RD1)–dependent manner [46]. Specifically, the ESX-1 secretion system was identified as the key RD1-encoded product responsible for mycobacterial release of DNA into the cytosol [37]. Thus, RD1, present in *M. tuberculosis* and *M. marinum* but absent from all BCG strains [47] contributes to the release of mycobacterial DNA into the cytosol.

The paragon cytoplasmic intracellular bacterium is *L. monocytogenes*, which replicates in the cytosol of infected host cells [34]. The *Listeria* protein Hly mediates bacterial egression into the cytosol, and accordingly, cytosolic localization of DNA has been demonstrated in the listeriosis model [15]. By integrating the *hly* gene into BCG and deleting urease C to allow establishment of an acidic pH optimum for Hly, rBCG was endowed with phagosome-perforating activity [23, 25, 29]. Evidence has been presented to suggest that rBCG perforates the phagosomal membrane, thus allowing release of vaccine antigens into the cytosol of host cells [23, 25, 29]. Perforation of

Table 3. Pathway Analysis of Genes Upregulated Exclusively in Recombinant BCG–Vaccinated Mice Versus Unvaccinated Mice

Pathway	*P* Value
Chemokine signaling pathway	4.275×10^{-9}
Cytokines and inflammatory response	.0015
Type II interferon signaling	.0021
Interleukin 1 signaling pathway	.0026
Complement and coagulation cascades	.0070
Peptide GPCRs	.0091
GPCRs, class A rhodopsin like	.0111
Toll-like receptors	.0481
Leptin-insulin overlap	.0030
Blood clotting cascade	.0400
GPCRs, class B secretin like	.0440
Interleukin 9 signaling pathway	.0481

A *P* value of < .05 is considered statistically significant.
Abbreviation: GPCR, G protein-coupled receptor.

the rBCG-harboring phagosome by Hly could play a key role in facilitating the release of mycobacterial DNA into the host cytosol, similar to ESX-1 in *M. tuberculosis* or *M. marinum* [37, 46]. Intriguingly, guanylate-binding proteins (GBPs) foster lysis of vacuoles containing gram-negative bacteria, leading to release of bacteria into the cytosol [48]. Consistent with these findings, elevated expression of *GBP2* and *GBP5* was observed in rBCG-infected THP-1 macrophages, compared with pBCG-infected macrophages (Supplementary Figure 3). It is therefore possible that GBP-facilitated lytic mechanisms participate in translocation of mycobacterial components from the vacuole into the cytosol in the case of rBCG. Intriguingly, *GBP* transcripts are part of a gene signature discriminating tuberculosis from latent *M. tuberculosis* infection [49].

In accordance with previous studies demonstrating involvement of AIM2 in the induction of autophagy [17], we identified elevated LC3-II levels after poly(dA:dT) stimulation. In addition, not only in AIM2 knockdown macrophages but also in STING knockdown macrophages, LC3-II levels upon pBCG or rBCG infection did not differ. Therefore, our results emphasize involvement of both AIM2 and STING in rBCG-induced autophagy. These 2 sensors may function in a nonredundant manner. Consistent with these in vitro data, we detected increased expression of 2 AIM2-related genes, *Ifi204* and *Pydc4*, and the STING-encoding gene *Tmem173* in lymph nodes of rBCG-vaccinated mice, but not pBCG-vaccinated mice, although we found virtually no increase in *Aim2* expression in mice vaccinated with rBCG. Autophagy promotes delivery of cytoplasmic antigens to MHC molecules for presentation to T cells [22]. Hence, we speculate that the superior protective immunity observed after vaccination with rBCG over pBCG [26] could, at least in part, be attributed to the induction of stronger autophagy by rBCG vaccination, compared with pBCG vaccination. Recent studies revealed that rBCG is a more potent inducer of Th17 cells and of central memory T cells than pBCG [26]. Future studies will investigate a potential link between autophagy and memory T-cell responses as potential correlates of protection against tuberculosis.

The rBCG vaccine candidate, termed VPM1002, has progressed through the clinical trials pipeline, to become the most advanced recombinant live tuberculosis vaccine [25]. Our findings described here provide several novel mechanistic insights into the cellular biology and subsequent immune events associated with this vaccine candidate by demonstrating that rBCG stimulated host innate immunity through AIM2 inflammasome activation and autophagy in vitro. Immunization strategies targeting these pathways could form a useful basis for rational design of novel tuberculosis vaccines either as replacement or as booster vaccines [50]. It will therefore be important to further elucidate how activation of these pathways translates into enhanced vaccine-induced protection mediated by T lymphocytes.

Supplementary Data

Supplementary materials are available at *The Journal of Infectious Diseases* online (http://jid.oxfordjournals.org). Supplementary materials consist of data provided by the author that are published to benefit the reader. The posted materials are not copyedited. The contents of all supplementary data are the sole responsibility of the authors. Questions or messages regarding errors should be addressed to the author.

Notes

Acknowledgments. We thank Mary Louise Grossman, for help in preparing the manuscript; Volker Brinkmann and Christian Goosmann, for advice and technical assistance regarding confocal microscopy; and Haipeng Liu, Gang Pei, and Alexis Vogelzang, for critical reading of the manuscript.

H. S., N. N., P. M.-A., A. D., and S. H. E. K. designed and supervised the study and wrote the manuscript; H. S., A.-B. K., and N. N. performed experiments and data analysis; M. G. and S. S. generated recombinant bacteria; P. M.-A. designed and produced knockdown cells; S. S. performed in vivo experiments; H.-J. M. and I. W. provided technical help for, and performed, microarray experiments; and all authors commented on the manuscript.

Financial support. This work was supported by the European Union's Seventh Framework Programme (EU FP7) Collaborative Projects NEW-TBVAC (HEALTH-F3-2009; grant 241745) and ADITEC (FP7/2007-2013; grant 280873) and the EU FP8 project TBVAC 2020 (grant 643381).

Potential conflicts of interest. S. H. E. K. is coinventor of the rBCG vaccine VPM1002. All other authors report no potential conflicts.

All authors have submitted the ICMJE Form for Disclosure of Potential Conflicts of Interest. Conflicts that the editors consider relevant to the content of the manuscript have been disclosed.

References

1. World Health Organization. Global tuberculosis report 2014. Geneva: WHO Press, **2014**.
2. Kaufmann SH. Envisioning future strategies for vaccination against tuberculosis. Nat Rev Immunol **2006**; 6:699–704.
3. Colditz GA, Brewer TF, Berkey CS, et al. Efficacy of BCG vaccine in the prevention of tuberculosis. Meta-analysis of the published literature. JAMA **1994**; 271:698–702.

4. Colditz GA, Berkey CS, Mosteller F, et al. The efficacy of bacillus Calmette-Guérin vaccination of newborns and infants in the prevention of tuberculosis: meta-analyses of the published literature. Pediatrics **1995**; 96:29–35.
5. Pieters J. *Mycobacterium tuberculosis* and the macrophage: maintaining a balance. Cell Host Microbe **2008**; 3:399–407.
6. Killick KE, Ní Cheallaigh C, O'Farrelly C, Hokamp K, MacHugh DE, Harris J. Receptor-mediated recognition of mycobacterial pathogens. Cell Microbiol **2013**; 15:1484–95.
7. Moura-Alves P, Faé K, Houthuys E, et al. AhR sensing of bacterial pigments regulates antibacterial defence. Nature **2014**; 512:387–92.
8. Kaufmann SH, Dorhoi A. Inflammation in tuberculosis: interactions, imbalances and interventions. Curr Opin Immunol **2013**; 25:441–9.
9. Cooper AM, Mayer-Barber KD, Sher A. Role of innate cytokines in mycobacterial infection. Mucosal Immunol **2011**; 4:252–60.
10. Schaible UE, Winau F, Sieling PA, et al. Apoptosis facilitates antigen presentation to T lymphocytes through MHC-I and CD1 in tuberculosis. Nat Med **2003**; 9:1039–46.
11. Martinon F, Mayor A, Tschopp J. The inflammasomes: guardians of the body. Annu Rev Immunol **2009**; 27:229–65.
12. Fernandes-Alnemri T, Yu JW, Datta P, Wu J, Alnemri ES. AIM2 activates the inflammasome and cell death in response to cytoplasmic DNA. Nature **2009**; 458:509–13.
13. Hornung V, Ablasser A, Charrel-Dennis M, et al. AIM2 recognizes cytosolic dsDNA and forms a caspase-1-activating inflammasome with ASC. Nature **2009**; 458:514–8.
14. Rathinam VA, Jiang Z, Waggoner SN, et al. The AIM2 inflammasome is essential for host defense against cytosolic bacteria and DNA viruses. Nat Immunol **2010**; 11:395–402.
15. Tsuchiya K, Hara H, Kawamura I, et al. Involvement of absent in melanoma 2 in inflammasome activation in macrophages infected with *Listeria monocytogenes*. J Immunol **2010**; 185:1186–95.
16. Saiga H, Kitada S, Shimada Y, et al. Critical role of AIM2 in *Mycobacterium tuberculosis* infection. Int Immunol **2012**; 24:637–44.
17. Shi CS, Shenderov K, Huang NN, et al. Activation of autophagy by inflammatory signals limits IL-1β production by targeting ubiquitinated inflammasomes for destruction. Nat Immunol **2012**; 13:255–63.
18. Shintani T, Klionsky DJ. Autophagy in health and disease: a double-edged sword. Science **2004**; 306:990–5.
19. Deretic V. Autophagy in tuberculosis. Cold Spring Harb Perspect Med **2014**; 4:a018481.
20. Gutierrez MG, Master SS, Singh SB, Taylor GA, Colombo MI, Deretic V. Autophagy is a defense mechanism inhibiting BCG and *Mycobacterium tuberculosis* survival in infected macrophages. Cell **2004**; 119:753–66.
21. Liu PT, Modlin RL. Human macrophage host defense against *Mycobacterium tuberculosis*. Curr Opin Immunol **2008**; 20:371–6.
22. Jagannath C, Lindsey DR, Dhandayuthapani S, Xu Y, Hunter RL Jr, Eissa NT. Autophagy enhances the efficacy of BCG vaccine by increasing peptide presentation in mouse dendritic cells. Nat Med **2009**; 15:267–76.
23. Grode L, Seiler P, Baumann S, et al. Increased vaccine efficacy against tuberculosis of recombinant *Mycobacterium bovis* bacille Calmette-Guérin mutants that secrete listeriolysin. J Clin Invest **2005**; 115:2472–9.
24. Grode L, Ganoza CA, Brohm C, Weiner J III, Eisele B, Kaufmann SH. Safety and immunogenicity of the recombinant BCG vaccine VPM1002 in a phase 1 open-label randomized clinical trial. Vaccine **2013**; 31:1340–8.
25. Kaufmann SH, Cotton MF, Eisele B, et al. The BCG replacement vaccine VPM1002: from drawing board to clinical trial. Expert Rev Vaccines **2014**; 13:619–30.
26. Vogelzang A, Perdomo C, Zedler U, et al. Central memory CD4+ T cells are responsible for the recombinant Bacillus Calmette-Guérin ΔureC:: hly vaccine's superior protection against tuberculosis. J Infect Dis **2014**; 210:1928–37.
27. Desel C, Dorhoi A, Bandermann S, Grode L, Eisele B, Kaufmann SH. Recombinant BCG ΔureC hly+ induces superior protection over parental BCG by stimulating a balanced combination of type 1 and type 17 cytokine responses. J Infect Dis **2011**; 204:1573–84.
28. Farinacci M, Weber S, Kaufmann SH. The recombinant tuberculosis vaccine rBCG ΔureC::hly(+) induces apoptotic vesicles for improved priming of CD4(+) and CD8(+) T cells. Vaccine **2012**; 30:7608–14.
29. Hess J, Miko D, Catic A, Lehmensiek V, Russell DG, Kaufmann SH. *Mycobacterium bovis* bacille Calmette-Guérin strains secreting listeriolysin of *Listeria monocytogenes*. Proc Natl Acad Sci U S A **1998**; 95:5299–304.
30. Stover CK, de la Cruz VF, Fuerst TR, et al. New use of BCG for recombinant vaccines. Nature **1991**; 351:456–60.
31. Tanida I, Ueno T, Kominami E. LC3 and autophagy. Methods Mol Biol **2008**; 445:77–88.
32. McIlwain DR, Berger T, Mak TW. Caspase functions in cell death and disease. Cold Spring Harb Perspect Biol **2013**; 5:a008656.
33. Tschopp J, Martinon F, Burns K. NALPs: a novel protein family involved in inflammation. Nat Rev Mol Cell Biol **2003**; 4:95–104.
34. Portnoy DA, Auerbuch V, Glomski IJ. The cell biology of *Listeria monocytogenes* infection: the intersection of bacterial pathogenesis and cell-mediated immunity. J Cell Biol **2002**; 158:409–14.
35. van der Wel N, Hava D, Houben D, et al. *M. tuberculosis* and *M. leprae* translocate from the phagolysosome to the cytosol in myeloid cells. Cell **2007**; 129:1287–98.
36. Stamm LM, Morisaki JH, Gao LY, et al. *Mycobacterium marinum* escapes from phagosomes and is propelled by actin-based motility. J Exp Med **2003**; 198:1361–8.
37. Manzanillo PS, Shiloh MU, Portnoy DA, Cox JS. *Mycobacterium tuberculosis* activates the DNA-dependent cytosolic surveillance pathway within macrophages. Cell Host Microbe **2012**; 11:469–80.
38. Lee H, Park HJ, Cho SN, Bai GH, Kim SJ. Species identification of mycobacteria by PCR-restriction fragment length polymorphism of the rpoB gene. J Clin Microbiol **2000**; 38:2966–71.
39. Watson RO, Manzanillo PS, Cox JS. Extracellular *M. tuberculosis* DNA targets bacteria for autophagy by activating the host DNA-sensing pathway. Cell **2012**; 150:803–15.
40. Adachi O, Kawai T, Takeda K, et al. Targeted disruption of the MyD88 gene results in loss of IL-1- and IL-18-mediated function. Immunity **1998**; 9:143–50.
41. Brunette RL, Young JM, Whitley DG, Brodsky IE, Malik HS, Stetson DB. Extensive evolutionary and functional diversity among mammalian AIM2-like receptors. J Exp Med **2012**; 209:1969–83.
42. Van de Craen M, Declercq W, Van den brande I, Fiers W, Vandenabeele P. The proteolytic procaspase activation network: an in vitro analysis. Cell Death Differ **1999**; 6:1117–24.
43. Akhter A, Gavrilin MA, Frantz L, et al. Caspase-7 activation by the Nlrc4/Ipaf inflammasome restricts *Legionella pneumophila* infection. PLoS Pathog **2009**; 5:e1000361.
44. Russell DG. *Mycobacterium tuberculosis* and the intimate discourse of a chronic infection. Immunol Rev **2011**; 240:252–68.
45. Müller I, Cobbold SP, Waldmann H, Kaufmann SH. Impaired resistance to *Mycobacterium tuberculosis* infection after selective in vivo depletion of L3T4+ and Lyt-2+ T cells. Infect Immun **1987**; 55:2037–41.
46. Smith J, Manoranjan J, Pan M, et al. Evidence for pore formation in host cell membranes by ESX-1-secreted ESAT-6 and its role in *Mycobacterium marinum* escape from the vacuole. Infect Immun **2008**; 76:5478–87.
47. Behr MA, Wilson MA, Gill WP, et al. Comparative genomics of BCG vaccines by whole-genome DNA microarray. Science **1999**; 284:1520–3.
48. Meunier E, Dick MS, Dreier RF, et al. Caspase-11 activation requires lysis of pathogen-containing vacuoles by IFN-induced GTPases. Nature **2014**; 509:366–70.
49. Weiner J III, Kaufmann SH. Recent advances towards tuberculosis control: vaccines and biomarkers. J Intern Med **2014**; 275:467–80.
50. Kaufmann SH. Tuberculosis vaccines: time to think about the next generation. Semin Immunol **2013**; 25:172–81.